



Detection of Gross Errors in Wellbore Directional Surveying for Petroleum Production with emphasis on Reliability Analyses

Erik Nyrnes, Torgeir Torkildsen, Hossein Nahavandchi

Vitenskapelig bedømt (refereed) artikkel

Erik Nyrnes & al.: Detection of Gross Errors in Wellbore Directional Surveying for Petroleum Production with emphasis on Reliability Analyses.

KART OG PLAN. Vol 65, pp. 1–19 P.O.B. 5003 N-1432 Ås, ISSN 0047-3278

This paper presents a method for the detection of gross errors in wellbore directional survey data. The method is general, and is applicable for both magnetic and gyroscopic surveys. However, this study will only examine magnetic surveys. The method is based on statistical tests and can be applied both in the single station estimation case or in connection with multi-survey processing techniques.

In contrast to other methods for error detection commonly used in the petroleum industry, which compare the measured gravity field strength, magnetic field strength and dip angle with values predicted from independent sources, this test is capable of detecting gross errors in any single sensor reading or reference component. By rejecting the corrupted measurements only, the new method brings an improvement to the quality of inclination and magnetic azimuth estimates.

The validity of such tests is shown to be dependent on several factors: Wellbore geometry, noise level in the measurements, estimation techniques, statistical significance and power. Based on synthetic data this is demonstrated by several examples to address two issues:

1. What is the critical error value, for each particular measurement, that may pass the test?
2. How much do potential undetected outliers affect the inclination and azimuth estimates?

These methods can detect errors that are 4 to 5 times greater than the nominal measurement noise levels. They are shown to be sharpest in connection with multi-survey processing techniques.

Key words: Wellbore surveying, Gross errors, Hypothesis testing, Data-snooping, Reliability analyses, Multi-station estimation, Single-station estimation.

Erik Nyrnes, PhD candidate, The Norwegian University of Science and Technology, Department of Civil and Transport Engineering, Division of Geomatics, Høgskoleringen 7G, N-7491 Trondheim. E-mail: erik.nyrnes@ntnu.no

Torgeir Torkildsen, Specialist, PhD, Statoil, Arkitekt Ebbells v 10, 7005 Trondheim. E-mail: torgeir.torkildsen@statoil.com

Hossein Nahavandchi, Associate professor, PhD, The Norwegian University of Science and Technology, Department of Civil and Transport Engineering, Division of Geomatics, Høgskoleringen 7G, N-7491 Trondheim. E-mail: hossein.nahavandchi@ntnu.no

1 Introduction

An accurate determination of the wellbore position is necessary in order to hit the planned targets and avoid collision or interference with existing wellbores. Wellbore po-

sitioning is performed by directional surveying tools which are run while drilling or on wirelines after drilling. The survey instruments commonly used in directional surveying consist of different sensors such as accel-

erometers, fluxgate magnetometers and mechanical gyroscopes. Measurements provided by the sensors are used to estimate the inclination, high side toolface and the azimuth. The inclination and high side toolface describe the orientation of the coordinate system of the survey tool with respect to the gravity field vector. The azimuth is used as the north reference. See Appendix A.1 for details.

A magnetic surveying tool consists of three accelerometers and three magnetometers which are used to measure orthogonal components of the local Earth's gravity and magnetic field vectors. The measurements are subject to errors which may be large or small. These are commonly divided into three classes such as systematic errors, random errors and gross errors (also called outliers). Gross errors, which seem to occur rather frequently in wellbore directional surveys, may produce erroneous results if they are not identified and removed. The cause of gross errors might be human blunders, software failures, sensor imperfections and environmental disturbances such as drillstring vibrations and large fluctuations in the Earth's magnetic field.

There are a number of different quality control procedures in the petroleum industry. One of these compares the measured gravity field strength, the magnetic field strength and dip angle with values predicted from independent sources [1]. If the deviations between the measured and predicted references exceed a specified acceptance limit, all measurements are rejected. The accelerometer and magnetometer readings are tested independently of each other.

A common way to check the measurements for potential outliers in linear regression analyses is to perform statistical testing of the residuals. Such tests originate from the theories of mathematical statistics. It will now be shown how they can be used in magnetic survey quality control applications.

The standard formulas (see Appendix A.1) used in the petroleum industry express the direct relation between equally weighted sensor readings and the inclination, toolface and azimuth estimates, which is a solution to

a nonlinear least squares problem. These equations process the measurements on a single survey station basis. Since the measurements are to be weighted differently and in order to account for the reference component uncertainties, the standard formulas are not useful in connection with the outlier detection procedures presented here. Instead the estimation is based on the method of Gauss-Newton, which has become a standard for geodetic and photogrammetric surveying applications. This approach will also be used to estimate the parameters on a multi-station basis and in connection with the single station axial magnetic correction technique (see Appendix A.1). The tests presented in this paper are capable of detecting gross errors in any single sensor reading and reference components. This is a great advantage since we then only reject the corrupted measurements and use the remaining ones to estimate the unknowns. The applicability of the error tests is demonstrated by reliability analysis. We use the minimum errors that can be detected with a given probability as a measure of this reliability. In geodetic and photogrammetric surveying this quantity is known as the internal reliability. It is further demonstrated how much these marginally detectable errors affect the inclination and azimuth estimates. This is known as the external reliability.

Most attention in this paper is on the detection of errors in single sensor readings. In this case potential outliers are modelled as unknown measurement biases. The procedure about how to detect systematic errors is also discussed. Systematic errors must also be seen as outliers as they constitute a common model misspecification for a group of measurements. An underlying assumption is that the conditions affecting the measurements do not vary significantly.

2 Statistical tests for the detection of outliers

2.1 General tests for outliers

First, we consider the linear regression model $E(\mathbf{y}) = \mathbf{X}\beta$, which in its augmented form reads:

Detection of Gross Errors in Wellbore Directional Surveying

$$E(\mathbf{y}) = [\mathbf{X} \ \mathbf{Z}] \begin{bmatrix} \boldsymbol{\beta} \\ \nabla \end{bmatrix} \text{ with Cov}(\mathbf{y}) = \Sigma_{ee} = \sigma^2 \mathbf{Q}_{ee} \quad (1)$$

where \mathbf{y} is a vector of n observations, $\boldsymbol{\beta}$ is a vector of u unknown fixed parameters, \mathbf{X} is an $n \times u$ design matrix, \mathbf{Z} is the $n \times r$ coefficient matrix corresponding to the r additional unknown model parameters ∇ , \mathbf{Q}_{ee} is a known observation error cofactor matrix and σ^2 is the variance of unit weight which is usually unknown. The errors \mathbf{e} are in this context assumed to be normally distributed, $\mathbf{e} \sim N(0, \Sigma_{ee})$. In wellbore positioning, the unknown additional parameters ∇ might represent sensor specific error terms such as scale factor, bias and sensor misalignment or unknown biases in individual measurements or groups of measurements. $\boldsymbol{\beta}$ may represent the angular components inclination I , tool-face τ , and magnetic azimuth A_m . These are often referred to as angular components. $\boldsymbol{\beta}$ and ∇ are estimated using a least squares adjustment approach. The following theories are from the linear algebra. However, if the observation equations are nonlinear, the estimation in the model (1) is based on linear approximations about initial values for the unknowns.

The test for the detection of outliers will be based on the following hypothesis:

$$H_0 : E(\mathbf{y}) = \mathbf{X} \boldsymbol{\beta} \text{ versus } H_A : E(\mathbf{y}) = [\mathbf{X} \ \mathbf{Z}] \begin{bmatrix} \boldsymbol{\beta} \\ \nabla \end{bmatrix}, \nabla \neq 0 \quad (2)$$

where H_0 is the null hypothesis that no model misspecification is present and H_A the alternative hypothesis that model misspecification ∇ is present. H_0 is rejected if the test statistic of the hypothesis exceeds a specified critical value of the current probability distribution, and otherwise accepted.

The outlier tests are performed as likelihood ratio tests by expressing the actual test statistic T of the above hypothesis as a function of the quadratic forms Ω and Ω_A of the residuals, computed under H_0 and H_A respectively. Ω can be considered as the constrained residual sum of squares, since it is

computed under the condition that the model errors ∇ are equal to zero.

It can be shown that, after specifying \mathbf{Z} , all computations concerning these tests can be performed under H_0 . The estimator $\hat{\nabla}$ for the model error ∇ can be expressed as:

$$\hat{\nabla} = (\mathbf{Z}^T \mathbf{Q}_{ee}^{-1} \mathbf{Q}_{\hat{e}_0 \hat{e}_0}^{-1} \mathbf{Q}_{ee}^{-1} \mathbf{Z})^{-1} \mathbf{Z}^T \mathbf{Q}_{ee}^{-1} \hat{e}_0 \quad (3)$$

where \hat{e}_0 is the H_0 residual vector and $\mathbf{Q}_{\hat{e}_0 \hat{e}_0}$ is the H_0 residual cofactor matrix. The subindex 0 to indicate H_0 is omitted from now on.

Under the normality assumption of the measurement errors \mathbf{e} and if σ^2 is known, the likelihood ratio test statistic T for the hypothesis of Equation (2) can be expressed as (see [3]):

$$T = R = \Omega - \Omega_A = \hat{\mathbf{e}}^T \Sigma_{ee}^{-1} \mathbf{Z} (\mathbf{Z}^T \Sigma_{ee}^{-1} \Sigma_{\hat{e}_0 \hat{e}_0}^{-1} \Sigma_{ee}^{-1} \mathbf{Z})^{-1} \mathbf{Z}^T \Sigma_{ee}^{-1} \hat{\mathbf{e}} \quad (4)$$

where $\Omega = \hat{\mathbf{e}}^T \Sigma_{ee}^{-1} \hat{\mathbf{e}}$ and $\Omega_A = \hat{\mathbf{e}}_A^T \Sigma_{ee}^{-1} \hat{\mathbf{e}}_A$. This test statistic is central chi-squared distributed under H_0 , $T \sim \chi_r^2$, see [3].

If σ^2 is unknown, the test statistic of the hypothesis in Equation (2) becomes (see [2]):

$$T = \frac{R / r}{\Omega_A / (n - u - r)} \quad (5)$$

which under H_0 is central Fisher distributed, $T \sim F_{(r, n-u-r)}$. R is the difference between $\Omega = \hat{\mathbf{e}}^T \mathbf{Q}_{ee}^{-1} \hat{\mathbf{e}}$ and $\Omega_A = \hat{\mathbf{e}}_A^T \mathbf{Q}_{ee}^{-1} \hat{\mathbf{e}}_A$. The τ^2 test statistic can also be used to test the hypothesis in Equation (2), see [2]. This test statistic is based on the constrained residual sum of squares Ω computed under H_0 . It is defined as:

$$\tau^2 = \frac{(n - u)T}{n - u - r + rT} = \frac{R / r}{\Omega / (n - u)} \quad (6)$$

The difference R may in this case be written as:

$$R = \hat{\mathbf{e}}^T \mathbf{Q}_{ee}^{-1} \mathbf{Z} (\mathbf{Z}^T \mathbf{Q}_{ee}^{-1} \mathbf{Q}_{\hat{e}_0 \hat{e}_0}^{-1} \mathbf{Q}_{ee}^{-1} \mathbf{Z})^{-1} \mathbf{Z}^T \mathbf{Q}_{ee}^{-1} \hat{\mathbf{e}} \quad (7)$$

The relation between the τ -distribution and the Fisher-distribution follows from Equation (6). The one-dimensional version of τ defines the distribution of the standardized residual, see Equation (15), and will therefore be useful for the detection of errors in single sensor readings. The application of the τ -test is straightforward and easy to implement in software.

2.2 Statistical tests for outliers in single measurements

We now turn to the one-dimensional version of the likelihood ratio test. By opposing H_0 against H_A the hypothesis for the outlier test of a particular measurement is formulated as:

$$H_0 : E(y) = X\beta \quad \text{versus} \quad H_A : E(y) = [X \quad c_i] \begin{bmatrix} \beta \\ \nabla_i \end{bmatrix}, \nabla_i \neq 0 \quad (8)$$

where the vector c_i is given by:

$$c_i = [0 \dots 0 \quad 1 \quad 0 \dots 0]^T \quad (9)$$

and where "1" represents the specific observation to be tested.

The estimate $\hat{\nabla}_i$ of the model error ∇_i of observation y_i now becomes:

$$\hat{\nabla}_i = (c_i^T Q_{ee}^{-1} Q_{\hat{e}\hat{e}} Q_{ee}^{-1} c_i)^{-1} c_i^T Q_{ee}^{-1} \hat{e} \quad (10)$$

Two different situations are considered in the following: σ^2 known or σ^2 unknown.

2.2.1 σ^2 known

If the variance of unit weight σ^2 is known a priori, the one-dimensional version of the test statistic of Equation (4) is used (see [3]):

$$w_i = \frac{\hat{\nabla}_i}{\sigma_{\hat{\nabla}_i}} = \frac{c_i^T \Sigma_{ee}^{-1} \hat{e}}{\sqrt{c_i^T \Sigma_{ee}^{-1} \Sigma_{\hat{e}\hat{e}} \Sigma_{ee}^{-1} c_i}} \quad (11)$$

which is normally distributed:

$$H_0 : w_i \sim N(0,1) \quad H_A : w_i \sim N(\lambda,1) \quad (12)$$

and where the non-centrality parameter λ is given by:

$$\lambda = \sqrt{c_i^T \Sigma_{ee}^{-1} \Sigma_{\hat{e}\hat{e}} \Sigma_{ee}^{-1} c_i} \nabla_i \quad (13)$$

The nominator of Equation (11) is called the transformed residual vector. The denominator is its standard deviation.

$$\text{Re ject } H_0 \text{ if } |w_i| > k_{\alpha/2} \quad (14)$$

where $k_{\alpha/2}$ is the critical value and α the significance level. Rejection of H_0 implies that observation y_i is corrupted by an outlier.

2.2.2 σ^2 unknown

If σ^2 is unknown the one dimensional version of the test statistic defined in Equation (6) is used (see also [2]):

$$\tau_i = \frac{\hat{\nabla}_i}{\hat{\sigma}_{\hat{\nabla}_i}} = \frac{c_i^T P \hat{e}}{\sqrt{c_i^T P Q_{\hat{e}\hat{e}} P c_i}} \quad (15)$$

where $P = Q_{ee}^{-1}$ is the weight matrix of the observations.

$$H_0 : \tau_i \sim \tau_{(n-u-1,0)} \quad H_A : \tau_i \sim \tau_{(n-u-1,\lambda)} \quad (16)$$

$$\lambda = \sqrt{c_i^T P Q_{\hat{e}\hat{e}} P c_i / \sigma_A^2} \nabla_i \quad (17)$$

where σ_A^2 denotes the variance of unit weight under the alternative hypothesis H_A . The relation between the τ and Student's t -distribution follows from Equation (6):

$$\tau = \frac{\sqrt{n-u} t_{n-u-1}}{\sqrt{n-u-1 + t_{n-u-1}^2}} \quad (18)$$

If Q_{ee} is diagonal, the test statistic in Equation (15) becomes $\hat{e}_i / \hat{\sigma}_{\hat{e}_i}$, commonly known as Pope's test statistic [4].

2.2.3 The error detection procedure in practice

An outlier test should be applied to all measurements y_n in the data set, not only a single measurement y_i . If H_0 expresses that no outliers are present in the measurements, the significance level of the individual tests α_i can be approximated by α/n [2] in order to keep the type I error¹ probability equal to the significance level α of the test H_0 . Because α_i tends towards zero when n increases, a lower limit must be set to make the test applicable if n is large.

The procedure of screening all measurements successively is known as data snooping. Provided that only one gross error is present in the measurements, the corrupted measurement will always have the largest test statistic. However, it may be that more than one measurement is corrupted. The measurement with the largest test statistic is rejected first. Because an outlier in one measurement may be masked by an outlier in another measurement, it is a common practice to re-run the adjustment without the rejected measurement. Having done this, it may be that a second outlier this time will have enough effect on its test statistic. If this is the case, the previously rejected measurement may not have been corrupted. The correct strategy, as a final check, would then be to replace the first suspected measurement and repeat the adjustment once again. If at this time the first measurement has enough effect on its test statistic, both measurements must be considered corrupted. This procedure, which is called iterative data snooping, works well in practice if there are few outliers in the dataset.

3 Reliability

We now turn to the concept of reliability which is divided into internal and external reliability. A measure of the internal reliability is the minimum error that is possible to detect by the test for outliers, while external reliability expresses how strongly these potential errors affect the estimated parameters.

3.1 Internal reliability

For a test with significance level α_i , there is for each particular measurement y_i a minimum error value ∇_0 which can be detected with probability β^2 . Consider the test statistic defined in Equation (11). The minimum detectable error ∇_0 in measurement y_i is found by solving (13) with respect to ∇ :

$$\nabla_0 = \frac{\lambda}{\sqrt{c_i^T \Sigma_{ee}^{-1} \Sigma_{\hat{c}\hat{c}} \Sigma_{ee}^{-1} c_i}} \tag{19}$$

The non-centrality parameter λ must be set according to the selected probability levels α and β for the actual test.

If the measurements are uncorrelated this expression simplifies to:

$$\nabla_0 = \sigma_i \frac{\lambda}{\sqrt{r_{ii}}} \tag{20}$$

where σ_i is the a priori standard deviation of the measurement y_i and r_{ii} is the corresponding redundancy number, i.e. the i 'th diagonal element in the redundancy matrix \mathbf{R} :

$$\mathbf{R}_{n \times n} = (\mathbf{Q}_{ee} - \mathbf{X}(\mathbf{X}^T \mathbf{P} \mathbf{X})^{-1} \mathbf{X}^T) \mathbf{P} = \mathbf{Q}_{\hat{c}\hat{c}} \mathbf{P} \tag{21}$$

A redundancy number r_{ii} expresses how strongly the true error e_i is reflected in the corresponding residual \hat{e}_i . The trace of \mathbf{R} equals the overall redundancy $n-u$ ($\text{trace}(\mathbf{R}) = n-u$) and is a global measure of reliability.

The measurement errors \mathbf{e} are assumed to be uncorrelated from now on. In this case the redundancy numbers \mathbf{r} vary between 0 and 1. As can be seen from Equation (20), observations with redundancy numbers close to zero can hardly be discovered by residual analysis since this causes ∇_0 to become large. Only a minor part of the outliers are detected in the residuals.

In geodetic and photogrammetric surveying applications, inspection of redundancy numbers can be used in the pre-analysis to discover portions of weak geometry and decide whether additional observations might be required. In wellbore directional survey-

ing, this decision must be made in real time, since it is not possible to predict the tool face angle. If the orientation of the survey instrument provides weak geometry, a correct action would be to perform a new survey. Both sets of measurements can then be used to improve the reliability.

Observations with small contributions to the redundancy (i.e. small r_{ii}) represent leverage points [2]. In linear regression analysis, a leverage point can be regarded as a data point that lies far away from the majority of the rest of the data points. Because $\hat{e}_i = x_i\hat{\beta} - y_i$, outliers in leverage points induce large biases in the estimates. When fitting a straight line through the data by the least squares method, an error in the leverage point will have a considerable effect on the tilt of the fitted line.

An example is when surveying a wellbore close to the horizontal east-west direction. In such attitudes the redundancy r of the along hole measurement \mathbf{b}_z tend towards zero, meaning that possible outliers have to be very large to be detected. An estimated bias \hat{V}_{bz} will tend to become very uncertain and the residual of the measurement \hat{e}_{bz} will tend to become very small. An axial error e_{bz} mainly affects the azimuth estimate in such directions. However, errors in the cross-axial measurements will have minor influence, since the corresponding redundancy numbers tend towards one. (See Appendix A for definition of coordinate systems.)

It is demonstrated in Figure 1 how an axial accelerometer bias ∇_{gz} of 5 Gal affects the x- and z-axis residuals \hat{e}_x, \hat{e}_z at different inclinations. The effects on the inclination estimates are also shown. The wellbore is surveyed with a toolface of 45 degrees and the transverse measurements $\mathbf{g}_x, \mathbf{g}_y$ are without any errors. The Earth's gravity field G is set to 980 Gal. Only the least squares residuals \hat{e}_x and \hat{e}_z are sketched, and not \hat{e}_y , since it is equal to \hat{e}_x . The figure shows that a residual \hat{e}_z absorbs a greater portion of ∇_{gz} in vertical positions than horizontally. The error ∇_{gz} may influence \hat{e}_x even more than \hat{e}_z in the nearly horizontal parts. However, the error has no effect on \hat{e}_z and \hat{e}_x when the wellbore is exactly horizontal, the residuals are zero. Errors in the axial accelerometer measure-

ments \mathbf{g}_z affect the inclination estimates most in horizontal attitudes.

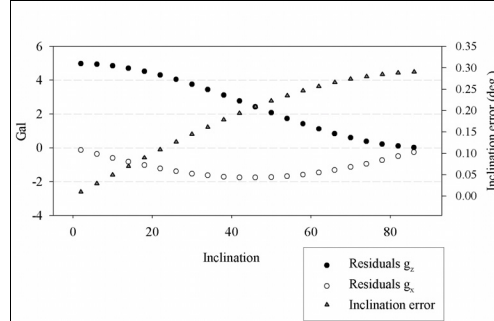


Figure 1: Left axis: The residuals \hat{e}_x and \hat{e}_z caused by ∇_{gz} (5 Gal). Right axis: Corresponding inclination errors.

Attention should be paid when visually scanning residual plots for possible outliers. As demonstrated above, it may be that the observation with the smallest residual has the largest error.

3.2 External reliability

A measure of the external reliability is how strongly the minimum detectable errors ∇_0 affect the estimated parameters. An external reliability vector, each of dimension u (the number of elements in β) is generated for each observation. An overall measure may be the largest effect caused by ∇_0 , which is not necessarily due to the observation with the largest ∇_0 .

An alternative approach is to define the external reliability tolerance, the maximum bias in the estimated parameters that is acceptable, and eliminate only those observations that cause the external reliability to be greater than the specified tolerance. An example of this approach is given in Section 5.2.

4 Measurement properties and estimation approaches

4.1 Sensor readings

The measurements from a specific sensor are corrected for various temperature and pressure dependent calibration parameters prior to the inclination, toolface and azimuth cal-

Detection of Gross Errors in Wellbore Directional Surveying

culations. Such parameters are mainly bias, linear scale factor ν and sensor misalignment α , and partly second order effects. Since these are random variables, random biases will remain in the measurements. The Industry Steering Committee on Wellbore Survey Accuracy (ISCWSA) has developed error models for magnetic directional surveys, which now have become an industry standard. These error models consider the combined effects of the residual errors, which can be shown to be modeled by a bias η and scale factor error ν , see [5].

Theoretically, the residual errors for a sensor reading $\xi = [\eta \ \nu]^T$ with uncertainties σ_η and σ_ν will be constant as long as the same sensor is in use. In addition, errors of environmental disturbances and sensor imperfections are present. For the specific sensor reading, these errors are lumped into a common error term e , which is also assumed to be random. The error properties of the sensor readings obtained from consecutive survey stations can then be based on the following assumptions:

- The elements in ξ are normally distributed, $\xi \sim N(0, \Sigma_{\xi\xi})$, mutually uncorrelated and totally correlated between consecutive measurements.
- The errors e are normally distributed with equal variances along the wellbore, $e \sim (0, \sigma_e^2 \mathbf{I})$.
- ξ and e are uncorrelated, $\xi \sim N(0, \Sigma_{\xi\xi})$.

In addition the error terms are assumed to be uncorrelated between the sensors. ξ are often referred to as systematic errors. Note however that ξ may include all kinds of sensor reading errors, and not necessarily those of the ISCWSA standard, but for instance error terms estimated in the calibration process.

The variance σ_e^2 should represent the average noise level in real survey data, if it is to be used in tests for the detection of outliers.

4.2 The Earth's reference components

Outliers in the reference components can also be detected if they are treated as measurements. Different sources can be used to predict their values.

The Earth's gravity field strength can be predicted using the international gravity formula. After corrections for local anomalies, the gravity can be predicted at any depth. See for instance [6] for details.

Reference components related to the Earth's magnetic field consist of a systematic term describing variations in the Earth's local crust and main field, and a random term describing external effects (temporal field). Components of the main field are provided by BGGM (British Geological Survey's Global Geomagnetic Model). This model can be improved on by measurement of the local crustal field, a technique often referred to as In Field Referencing (IFR). Improved In Field Referencing (IIFR) provides further improvements by correcting for the temporal field.

Statoil has developed its own accepted uncertainty levels for the different references. One such is the Statoil Accepted Enhanced Reference, which represents the IFR conditions.

4.3 Estimation approaches

4.3.1 Multi-Station Estimation (MSE)

Multiple surveys from several survey stations can be used to estimate and account for systematic error terms on all measurements, see [7] for details. These techniques will be referred to as Multi-Station Estimation (MSE). Such techniques can also be used to process multiple surveys on the same station, for example when performing rotational shots or check shots. The outlier detection in connection with MSE is either based on the known variance σ^2 or its estimate $\hat{\sigma}^2$, see Section 2.2. Note however that the estimation in the model (1) is based on the known weight relations \mathbf{P} .

4.3.2 Single Station Estimation (SSE)

Ignoring all covariances, the variance σ_{ii}^2 of an individual measurement y_i follows by the law of variance propagation:

$$\sigma_{ii}^2 = \sigma_\eta^2 + (\sigma_\nu y_i)^2 + \sigma_e^2 \tag{22}$$

where σ_η^2 and σ_ν^2 are the variances of the bias and scale residual errors and σ_e^2 the variance of the uncorrelated errors e .

The standard formulas (see Appendix A.1) are not functions of the Earth's gravity and magnetic field reference components. However, the reference errors affect the residuals $\hat{\mathbf{e}} = \mathbf{y} - \hat{\mathbf{E}}(\mathbf{y})$.

For example, an error dG in the local gravity G affects the residuals $\hat{\mathbf{e}}$ according to:

$$d\hat{e}_x = -\sin I \sin \tau dG \quad (23)$$

$$d\hat{e}_y = -\sin I \cos \tau dG \quad (24)$$

$$d\hat{e}_z = \cos I dG \quad (25)$$

which means that $d\hat{e}_x$ and $d\hat{e}_y$ increase with greater inclination while $d\hat{e}_z$ decreases when approaching the vertical.

Standard formulas are not considered useful for detecting outliers. Instead, the least squares estimation in connection with MSE and SSE is based on the Gauss-Newton method. It will then be easy to weight the sensor readings differently, including the measurements of reference components (G , B and Θ).

5 Numerical investigations

Finally, the reliability of the outlier tests, in terms of critical error values and corresponding inclination and azimuth impacts, is demonstrated on magnetic surveys. The error values are calculated for various measurement categories in connection with MSE and two different SSE techniques (with and without axial magnetic correction, see Appendix A.1). The estimation is based on the functional models given in Appendix A.3.

5.1 Basic assumptions.

The reliability analyses are based on the uncertainties (standard deviations) in Table 1 (there are some exceptions, see Section 5.2).

5.1.1 Sensor specific uncertainties

The systematic sensor specific error uncertainties, which are relevant when SSE is applied, are set in accordance with the ISCWSA standard. The axial magnetometer uncertainty $\sigma_{\eta_{bz}}$ is the lumped uncertainties of sensor specific errors (70nT) and axial mag-

netic interference (≈ 150 nT). See Table 1 for details.

For all estimation approaches, the effects of random environmental errors (magnetic reference errors, drillstring vibrations etc.) are lumped together with other sources of random sensor specific errors to create the uncertainty terms σ_{e_g} and σ_{e_b} of the accelerometer and magnetometer readings respectively. It has been confirmed by analyses of magnetic survey data that these error values reflect reality.

Sensor reading uncertainties in connection with the SSE reliability analyses are derived using Equation (22). The first two terms are in accordance with the ISCWSA standard. The third term is the white noise variance. See Table 1 for details.

5.1.2 Reference component uncertainties

The reference components are treated as measurements throughout the analyses and are common references for all sensor readings in the MSE case. They will have the most significant influence when the estimation is carried out on an SSE basis. The magnetic field uncertainties σ_B and σ_Θ are set equal to the Statoil Accepted Enhanced Reference (IFR). The standard deviations σ_G , σ_B , σ_Θ of systematic reference component errors are shown in Table 1. The gravity field is given the worst case uncertainty.

5.1.3 Other relevant information

All the measurements in the analyses are processed as being uncorrelated (i.e. Σ_{ee} diagonal). Since σ^2 is a known parameter, the results are in accordance with the application of the test statistic [2]:

$$\delta_i = \frac{\hat{e}_i}{\sigma_{\hat{e}_i}} \quad (26)$$

where \hat{e}_i is the residual and $\sigma_{\hat{e}_i}$ its standard deviation. This normalized residual is known from geodetic and photogrammetric surveying as Baarda's test statistic. It can be considered as a simplification of the test statistic w_i in Equation (11) if the measurement errors are known to be correlated. Equation (20) has been used to calculate the internal reliability.

Detection of Gross Errors in Wellbore Directional Surveying

When MSE is applied to a large number of survey stations, the introduction of a few systematic error terms will not have significant effects on individual redundancy numbers r_{ii} . As a result, we only consider the random measurement errors \mathbf{e} , see Table 1.

The test H_0 , that no outliers are present in the measurements, is based on the total significance level = 0.05 (5%) and the power $\beta = 0.8$ (80%).

The plots in Figures 3–6 can be interpreted to answer this question: For a given surveying tool attitude (I , τ and A_m) and a test size β , how large must an error ∇ in the measurement y_i at least be in order to be detected with probability β ?

Uncertainties (σ)	SSE	MSE
σ_G	0.3 Gal	0.3 Gal
σ_B	65 nT	65 nT
σ_θ	0.12 deg	0.12 deg
$\sigma_{\eta\beta}$	70 nT	0
$\sigma_{\nu\beta}$	0.16 %	0
$\sigma_{\eta bz}$	$\sqrt{(150 \text{ nT})^2 + (70 \text{ nT})^2}$	0
σ_{eb}	70 nT	70 nT
$\sigma_{\eta g}$	0.39 Gal	0
$\sigma_{\nu g}$	0.05 %	0
σ_{eg}	0.3 Gal	0.3 Gal

Table 1: Uncertainties (1σ) used in reliability analysis. Units: Gal. (1 Gal = 0.01m/s²), nT (nanoTesla). $G = 982$ Gal, $B = 51000$ nT.

5.2 Reliability analysis of the accelerometer measurements

The reliability of the along hole accelerometer sensor is investigated for the wellbore in Figure 1, without introducing magnetometer measurements. Two estimation approaches are considered, SSE and MSE. The external reliability tolerance error is set to 0.1 degrees. The final borehole inclination error might exceed 0.1 degrees when all significant error sources are taken into account.

In addition to the values displayed in Table 1, the MSE reliability analysis also in-

volves a second uncertainty level for white noise of 0.15 Gal ($\sigma_e = 0.15$ Gal). The interval 0.15-0.3 Gal is a reasonable noise level.

The variances used in the SSE reliability analysis are derived from Equation (22). The significance level α_i is set to 0.00025, which should lead to an approximate type I error probability of 0.05 for a wellbore of 30 survey stations.

5.2.1 Example

Consider three accelerometer measurements $\mathbf{y} = [g_x \ g_y \ g_z]^T$ with a priori statistical properties $\Sigma_{ee} = \sigma^2 \mathbf{I}$. The functional models of these measurements are given in Appendix A.3. After forming the elements of \mathbf{X} (which consist of partial derivatives), the elements in the covariance matrix of the residuals $\Sigma_{\hat{e}\hat{e}} = \sigma^2 \mathbf{R}$ become $\sigma^2(\mathbf{I} - \mathbf{X}(\mathbf{X}^T \mathbf{X})^{-1} \mathbf{X}^T)$:

$$\sigma_{\hat{e}_x}^2 = \sigma^2 \sin^2 I \sin^2 \tau \tag{27}$$

$$\sigma_{\hat{e}_y}^2 = \sigma^2 \sin^2 I \cos^2 \tau \tag{28}$$

$$\sigma_{\hat{e}_z}^2 = \sigma^2 \cos^2 I \tag{29}$$

$$\sigma_{\hat{e}_x \hat{e}_y} = \sigma^2 \sin^2 I \sin \tau \cos \tau \tag{27}$$

$$\sigma_{\hat{e}_x \hat{e}_z} = -\sigma^2 \cos I \sin \tau \sin I \tag{28}$$

$$\sigma_{\hat{e}_y \hat{e}_z} = -\sigma^2 \cos I \cos \tau \sin I \tag{29}$$

From these expressions it follows that the absolute values of the correlation coefficients $|\rho_{\hat{e}_x \hat{e}_y}| = |\rho_{\hat{e}_x \hat{e}_z}| = |\rho_{\hat{e}_y \hat{e}_z}| = 1$, thus the residuals $\hat{\mathbf{e}}$ become fully correlated irrespective of the geometry. As a further example, consider the measurement g_x affected by the error e_x of magnitude ∇ . Because $\mathbf{R} = (1/\sigma^2)_{\hat{e}\hat{e}}$ in this case, the impacts $d\hat{\mathbf{e}}_x$ become:

$$d\hat{\mathbf{e}}_x = \frac{1}{\sigma^2} \begin{bmatrix} \sigma_{\hat{e}_x}^2 \nabla & \sigma_{\hat{e}_x \hat{e}_y} \nabla & \sigma_{\hat{e}_x \hat{e}_z} \nabla \end{bmatrix}^T \tag{33}$$

Using the expressions in the Equations (27)-(32), the absolute values for the test statistics δ in Equation (26) become equal for all three, namely $\sigma^{-1} \nabla \sin I \sin \tau$. Rejection of H_0 is

just an indication of model misspecification and it is not possible to pinpoint the corrupted measurement since the redundancy is one. Theoretically, this situation improves when the adjustment also includes magnetometer measurements, since these also are inclination and toolface dependent, see Appendix A.3.

5.2.3 Results

Both the internal and external reliability for the axial sensor readings are shown in Figure 2. The upper left plot shows the minimum detectable error ∇_0 at different inclinations. Two of the curves represent ∇_0 for the MSE at the noise levels $\sigma_e = 0.15$ Gal and $\sigma_e = 0.3$ Gal. SSE provides the poorest reliability.

The upper right plot shows the corresponding external reliability, expressed as inclination biases caused by each ∇_0 . The lower plot in Figure 2 compares the internal reliability and the external reliability tolerance, the maximum error in the measurement that is acceptable to keep the inclination bias on that particular station at maximum 0.1 degrees. According to the breaking points, represented by the intersections of the curves, these tests should not be used in connection with SSE if the inclinations exceed 35 degrees. When it comes to MSE, the situation improves considerably, the breaking point for the lowest noise level ($\sigma_e = 0.15$ Gal) almost reaches an inclination of 70 degrees.

Reliability levels, axial accelerometer measurements.
Single and Multi Station Estimation.

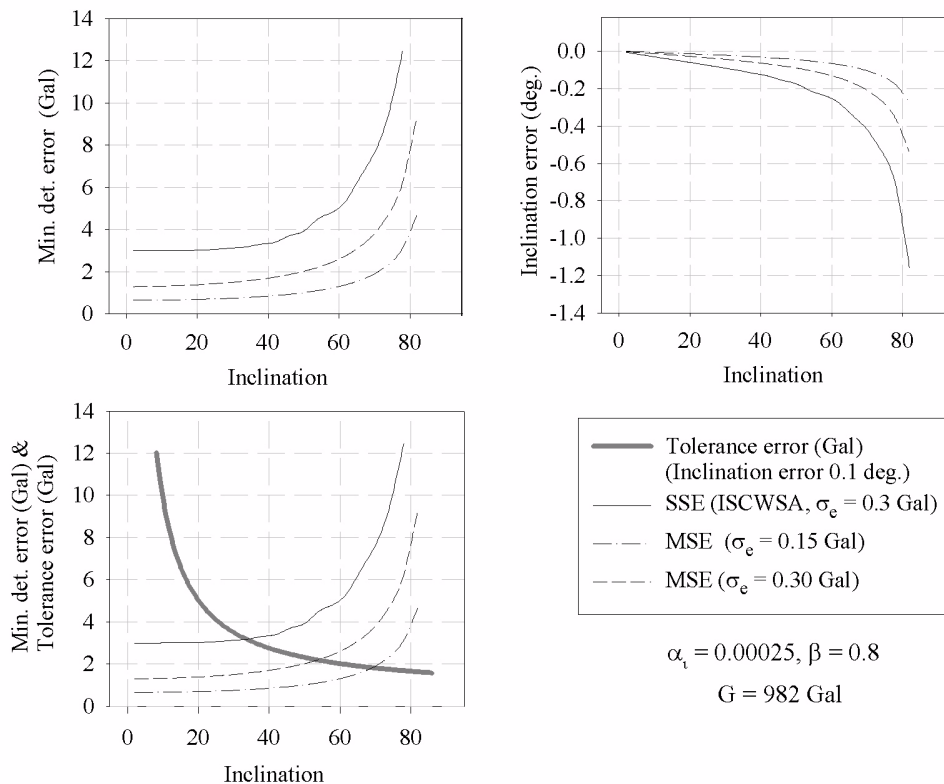


Figure 2: Upper left plot: Internal reliability, g_z . Upper right plot: External reliability, g_z . Lower left plot: Comparison between tolerance error and internal reliability. The tests are not useful when the inclination passes the breaking point.

Detection of Gross Errors in Wellbore Directional Surveying

5.3 Reliability analysis of the magnetometer measurements

From a theoretical point of view, the combined adjustment of accelerometer and magnetometer makes it possible to detect outliers in individual accelerometer readings. This ability is dependent on several factors, among them the weight relations, tool attitude and wellbore direction. Experience with survey data from the North Sea imply that the noise levels in magnetometer measurements must be considered higher than accelerometer measurements. This is mainly due to the fact that the Earth's magnetic field is a much more unstable reference than the Earth's gravity field, and partly because magnetic sensors are noisier in principle. Because of this, magnetometer measurements do not necessarily make any large contribution to the inclination estimation or to the detection of errors in accelerometer measurements. The contribution is also geometry dependent.

Case	α_i	β	I	τ	A_m
1-3	0.0001	0.8	30 & 70	0-180	0-180
4	0.0001	0.8	0-180	-	0-180

Table 3: Angular components (deg.) and probability levels. ($\Theta = 75$ deg.)

The combined adjustment involves nine measurements (sensor readings and reference components) at each station for the SSE, while the MSE involves six on average. Using the approximation $\alpha_i = (\alpha/2)/n$, the individual significance levels for the two approaches will hardly differ for longer wellbores. Cases 1-4 below consider a wellbore consisting of 30 stations. The test size α_i is set to 0.0001 (0.01%) to make the type I error probability approximately 0.05 (5%). Using synthetic measurements, the reliability of the outlier tests is demonstrated for the following estimation approaches:

1. Cross-axial magnetometer readings (b_x, b_y), SSE.
2. Cross-axial magnetometer readings (b_x, b_y), SSE with axial magnetic correction.
3. Cross-axial magnetometer readings (b_x, b_y), MSE.

4. Axial magnetometer readings (b_z), SSE and MSE.

The internal and external reliabilities are illustrated by different contour plots in Figures 3-6. The external reliabilities are in absolute values. The dip angle Θ is 75 degrees, an average for the North Sea and Norwegian Ocean area. The error values are for the x-axis measurements b_x given for varying magnetic azimuth A_m and toolface τ angles at two different inclinations, $I = 30$ and $I = 70$ degrees. The pattern is repeated at 180 degrees and can therefore be used to study the reliability for toolfaces and azimuths up to 360 degrees. For the z-axis measurements b_z the error values are shown for inclinations up to 90 degrees. See Table 2 for details.

Figures 3-6 can be used to study the reliability of the y-axis measurements b_y as well, simply by shifting the toolface angle 90 degrees.

The reliability analyses are based on the information in Tables 1 and 2. When other sources of errors, such as errors in the magnetic declination and instrument misalignments in the borehole are taken into consideration, the total azimuth uncertainty might exceed 1 degree. An external reliability tolerance of 1 degree is therefore assumed to be reasonable.

5.3.1 Comments on the results

The results are as follows:

Case 1. Cross-axial magnetometer readings (b_x, b_y) in ordinary SSE mode.

The plots on the left side of Figure 3 show that the minimum detectable error ∇_0 tends towards infinity when the azimuth A_m and the toolface τ is simultaneously close to either 0 or 180 degrees (see the areas around the corners of the plots). The reliability is poorest for the steepest wellbore ($I = 30$ degrees). The largest difference occurs when τ and A_m both are 90 degrees. The reliability improves considerably for these attitudes when the inclination is 70 degrees (see the lower left plot).

The lowest values for the ∇_0 are approximately 650 nT for both inclinations (this value is not shown for the steepest wellbore).

The external reliability levels are shown to the right in Figure 3. It is worth noting that the azimuth errors tend towards zero along individual curves, which is where the measurement has no influence on the azimuth estimation. It can be seen from the plots that the azimuth errors are almost six times larger for the steepest wellbore. In general, the ability to detect outliers on the cross-axial measurements \mathbf{b}_x , \mathbf{b}_y improves when approaching the horizontal. When the inclination is 70 degrees, a large amount of the azimuth errors are smaller than the external reliability tolerance of 1 degree.

Case 2. Cross-axial magnetometer readings (\mathbf{b}_x , \mathbf{b}_y) in SSE mode with axial magnetic correction.

The results are given in Figure 4. Since this estimation approach ignores the axial measurement b_z in the azimuth calculation, the reliability of the cross-axial measurements $\mathbf{b}_x, \mathbf{b}_y$ is expected to be poorer than when applying SSE without axial correction (i.e. ordinary SSE). However, compared to the previous case (see Figure 3), the error values are quite similar for the steepest wellbore ($I = 30$ degrees). When ordinary SSE is applied under this condition, the axial measurements will have minor influence on the azimuth estimation, and thus the two methods produce similar results (reliability).

In contrast to the ordinary SSE approach, the overall reliability will not improve for the SSE with axial correction when approaching the horizontal. The lower left plot in Figure 4 shows that the reliability becomes poorer for some attitudes while it improves for others.

Because azimuth errors greater than the external reliability tolerance are very likely, SSE with axial correction generally provides poor reliability, even for wellbores close to the horizontal.

Case 3. Cross-axial magnetometer readings (\mathbf{b}_x , \mathbf{b}_y) in MSE mode.

Since this estimation approach can be used to account for systematic error terms on all measurements (by the introduction of additional parameters), only the random errors \mathbf{e} are considered. Because of this, MSE provides the best reliability. The results show

the same trends as the ordinary SSE reliability analysis, except that the error values are smaller. A comparison shows that the MSE leads to a 50 % reduction in the error values for both inclinations (30 and 70 degrees). According to Figure 5, the smallest values for the minimum detectable errors ∇_0 are approximately 350 nT.

However, under special conditions the MSE must be considered to provide a poor reliability, especially for steeper wellbores. When the inclination is 30 degrees, azimuth errors larger than 1 degree cover the major part of the external reliability maps.

Case 4. Axial magnetometer readings (\mathbf{b}_z) in SSE and MSE mode.

Figure 6 shows that the reliability of the axial sensor is poorest in horizontal east/west directions. This is in agreement with the well-known inability to apply axial magnetic correction algorithms in such directions. Vertical attitudes provide the best reliability for this sensor. However, b_z errors will leave \hat{A}_m totally unharmed in such positions.

The error tests provide the best reliability under MSE. The gross errors that might remain undetected are almost three times larger when SSE is applied.

6 Discussion and Conclusions

The ability to detect outliers in magnetic survey data, except for the cross-axial accelerometer readings, has been demonstrated by reliability analyses. The reliability, described by the minimum detectable errors and corresponding inclination and azimuth impacts, is shown to be strongly dependent on the actual surveying tool attitude (inclination, toolface and azimuth). However, it should be considered that reliability also depends on other factors; the actual stochastic model (Σ_{ee}), the significance level α , the power β and the degrees of freedom.

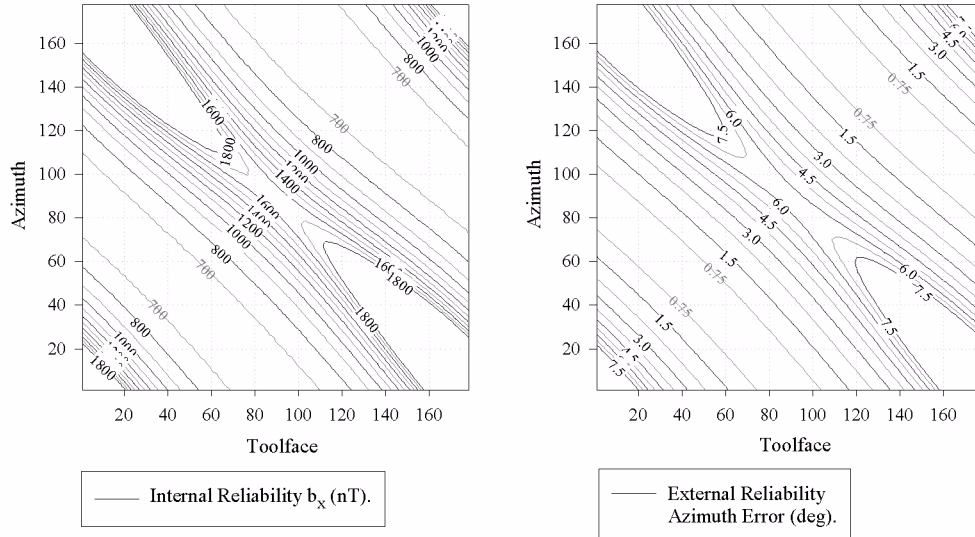
MSE (Multi-Station Estimation) was shown to provide the best reliability. In this case the outlier tests (with a power of 80 % and a significance level of a few tenth of per mille) were capable of detecting errors with magnitudes 4 to 5 times the nominal noise level of the sensor readings. As a compari-

Detection of Gross Errors in Wellbore Directional Surveying

Single Station Estimation Reliability Levels.

$$\alpha_t = 0.0001, \beta = 0.8$$

Inc. = 30 deg. Dip angle = 75 deg.



Inc. = 70 deg. Dip angle = 75 deg.

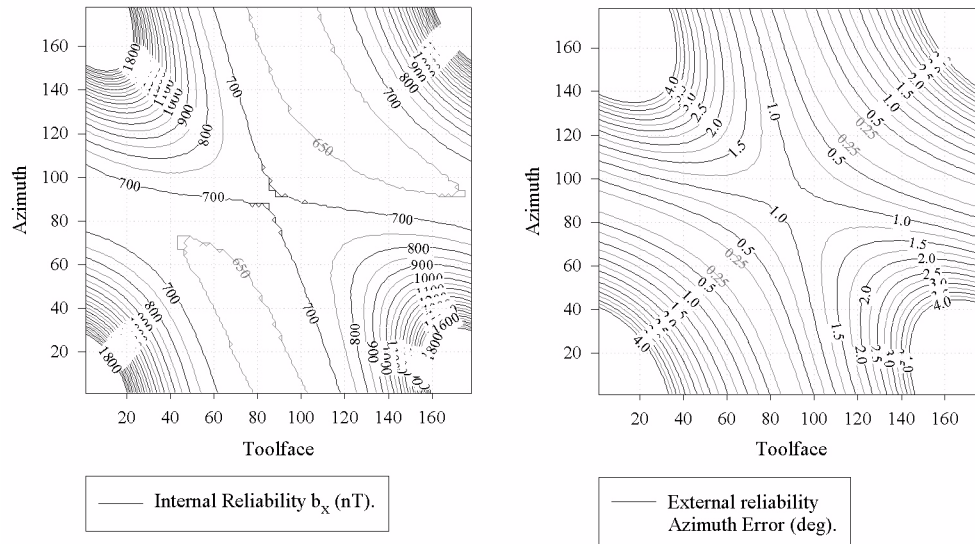


Figure 3: Internal and external reliability b_x , SSE.

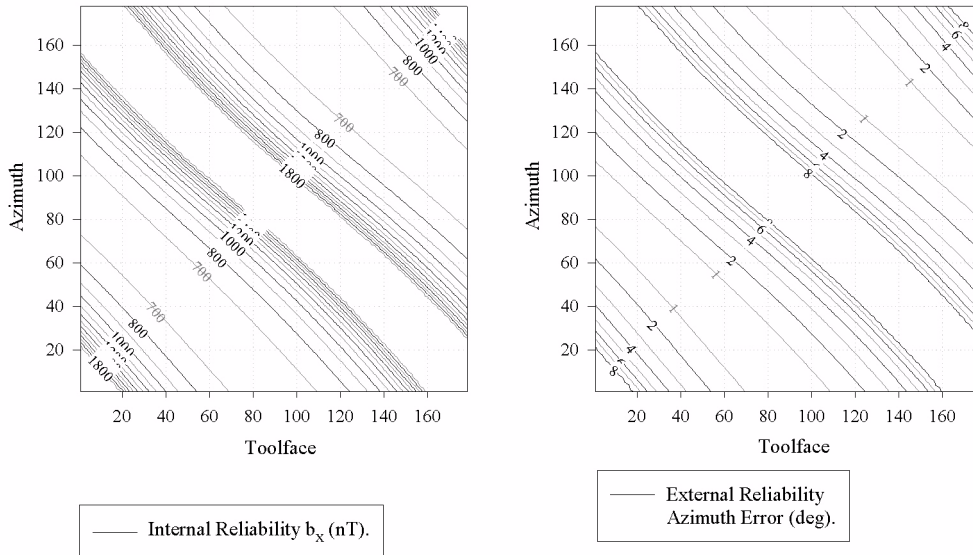
Erik Nyrnes, Torgeir Torkildsen, Hossein Nahavandchi

Single Station Estimation Reliability Levels.

Axial Mag. Correction

$$\alpha_1 = 0.0001, \beta = 0.8$$

Inc. = 30 deg. Dip angle = 75 deg.



Inc. = 70 deg. Dip angle = 75 deg.

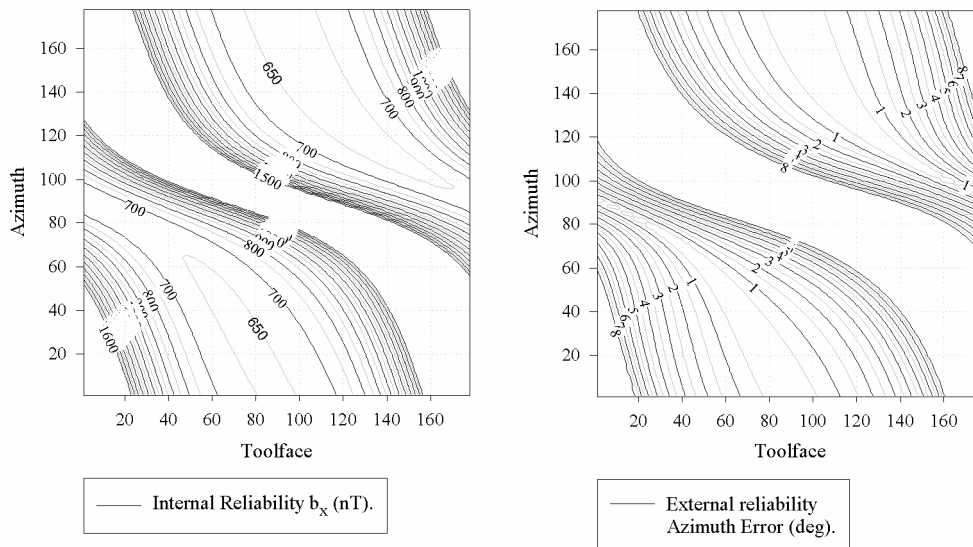


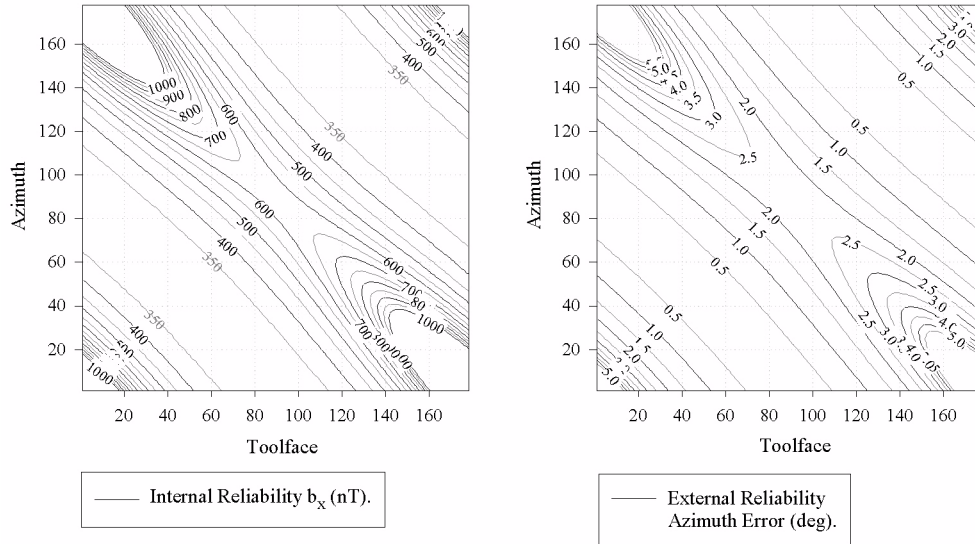
Figure 4: Internal and external reliability b_x , SSE, axial mag. correction.

Detection of Gross Errors in Wellbore Directional Surveying

Multi Station Estimation Reliability Levels.

$$\alpha_1 = 0.0001, \beta = 0.80$$

Inc. = 30 deg. Dip angle = 75 deg.



Inc. = 70 deg. Dip angle = 75 deg.

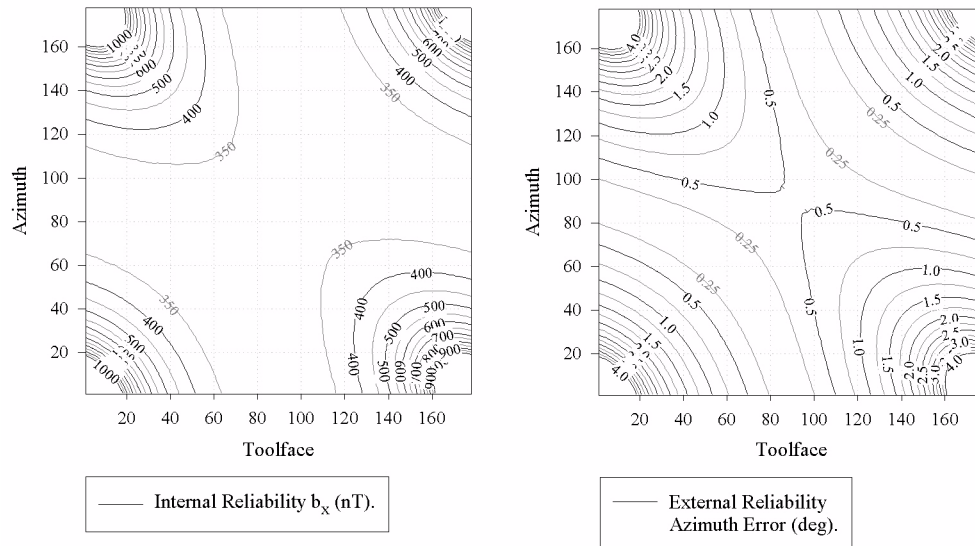


Figure 5: Internal and external reliability b_x , MSE.

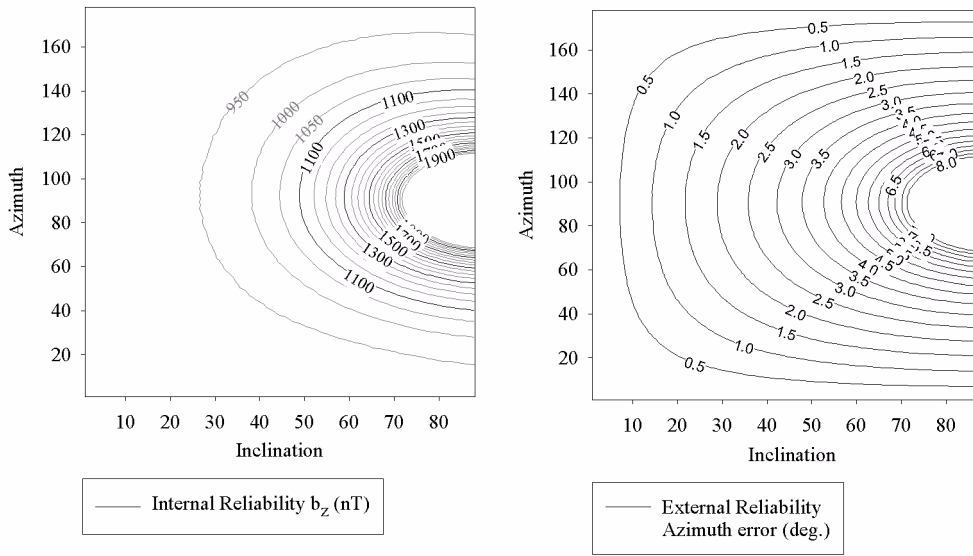
Erik Nyrnes, Torgeir Torkildsen, Hossein Nahavandchi

Reliability Analysis, axial magnetometer measurements.

Dip angle = 75 deg.

$\alpha_1 = 0.0001, \beta = 0.8$

Single Station Estimation.



Multi Station Estimation.

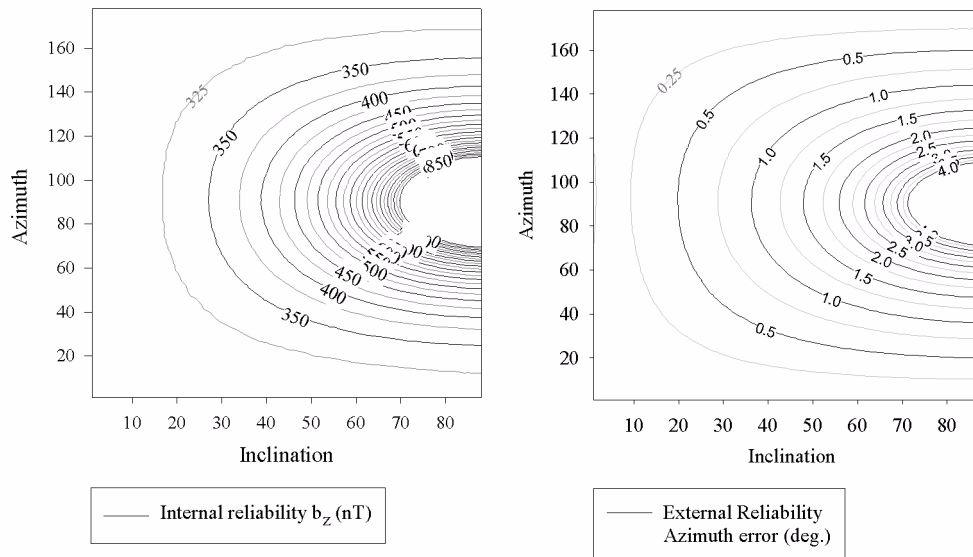


Figure 6: Internal and external reliability b_z , SSE and MSE.

Detection of Gross Errors in Wellbore Directional Surveying

son, the error values obtained by SSE (Single Station Estimation) were at least twice as large. The reliability generally improved for the cross-axial magnetometers when approaching the horizontal, while it tended to be better in steeper attitudes for the axial magnetometer. Vertical positions also provided the best reliability for the axial accelerometer readings.

The reliability analyses were based on realistic noise levels. The external reliability tolerance errors were also used as a measure of reliability. These error limits were set to 0.1 and 1 degrees for the inclination and azimuth estimates respectively. For the MSE, azimuth errors smaller than the external reliability tolerance could represent the majority of possible tool attitudes. The inclination errors caused by the minimum detectable axial accelerometer errors had to be as large as 70 degrees to exceed the 0.1 degree limit.

The SSE without axial correction was also shown to provide fairly good reliability, at least for attitudes close to the horizontal. However, this was not the case for SSE with axial magnetic correction. Azimuth errors exceeding the 1 degree level were very likely, even for horizontal positions.

The SSE also provided poor reliability for the axial accelerometer readings when the inclinations were greater than 35 degrees.

Appendix A: Coordinate systems and basic definitions
A.1 Coordinate systems

In wellbore surveying there are three different coordinate systems in common use; the orthogonal right handed instrument-based xyz system, the orthogonal right-handed local Earth-based North/East/Vertical NEV system and the magnetic reference system. See [8] for further details.

The vertical axis of the NEV system coincides with the plumb line and the north axis points towards true north. The xyz system has its z-axis aligned along the wellbore axis (i.e. the instrument collar).

The connections between xyz and NEV are given by the azimuth A, the inclination I and the high side toolface τ , see Figures 7 and 8. The NEV system is linked to the magnetic

reference system by the magnetic declination δ and magnetic dip Θ as shown in Figure 7. At a particular point, δ is defined as the angular difference between the horizontal component of the Earth's magnetic field vector and true north. It is by definition positive when magnetic north lies east of true north, and negative when magnetic north lies west of the true north.

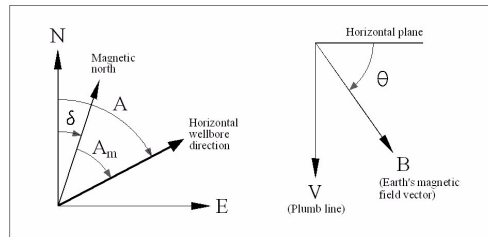


Figure 7: Definition of azimuth, magnetic azimuth, declination and magnetic dip angle.

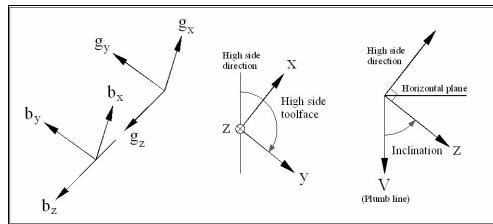


Figure 8: Definition of instrument xyz coordinate system, high side toolface and inclination.

The inclination I is defined as the vertical angle between the plumb line and the wellbore axis (z-axis). From the accelerometer readings (g_x, g_y, g_z) its least squares estimator is commonly calculated by:

$$\hat{I} = \frac{\sqrt{g_x^2 + g_y^2}}{g_z} \tag{34}$$

This equation is derived from equally weighted measurements. In the case of a two-accelerometer survey tool, the inclination is calculated using additional information about the local gravity field G.

High side direction is defined as the line of intersection between the vertical plane containing the z-axis and a plane perpendicular

to the z-axis. High side toolface τ is defined as the angular difference between the high side direction and the y-axis, and is given by:

$$\hat{\tau} = \arctan \frac{-g_x}{-g_y} \quad (35)$$

The true azimuth A is defined as the clockwise angle between the direction of true north and the horizontal projection of the z-axis. The magnetometer measurements (b_x, b_y, b_z) are used together with \hat{I} and $\hat{\tau}$ to calculate the magnetic azimuth estimate \hat{A}_m . The true azimuth estimate \hat{A} is commonly found by:

$$\hat{A} = \delta + \hat{A}_m = \delta + \arctan \frac{b_x \cos \hat{\tau} - b_y \sin \hat{\tau}}{\cos \hat{I} (b_x \sin \hat{\tau} + b_y \cos \hat{\tau}) + b_z \sin \hat{I}} \quad (36)$$

This equation is based on equally weighted magnetometer measurements and error free inclination and toolface estimates. Another approach for the azimuth estimation is applied if the drill string or the Bottom Hole Assembly (BHA), which the survey instrument is a part of, generates unacceptably high axial magnetic interference. This method ignores the z-axis measurement and uses information about the Earth's magnetic field components in the azimuth estimation.

A.2 Calculation of wellbore position

A commonly used method to calculate the wellbore position is the minimum curvature.

From the inclination and azimuth estimates, the relative position difference between the survey points $i-1$ and i , in terms of northing X_i , easting δY_i and vertical direction Z_i , can be calculated by (see [8]):

$$\begin{bmatrix} \delta X_i \\ \delta Y_i \\ \delta Z_i \end{bmatrix} = \frac{D_i - D_{i-1}}{2} \begin{bmatrix} \sin \hat{I}_{i-1} \cos \hat{A}_{i-1} + \sin \hat{I}_i \cos \hat{A}_i \\ \sin \hat{I}_{i-1} \sin \hat{A}_{i-1} + \sin \hat{I}_i \sin \hat{A}_i \\ \cos \hat{I}_{i-1} + \cos \hat{I}_i \end{bmatrix} \text{RF} \quad (37)$$

where $D_i - D_{i-1}$ is the measured length of the drill string between survey station i and $i-1$ and RF the minimum curvature ratio factor (which for a straight well is 1). For a wellbore of n survey stations the relative position of the n 'th point relative to the starting point is given by the sum of all the relative coordinate differences:

$$[X \ Y \ Z]_n^T = \sum_{i=1}^n [\delta X_i \ \delta Y_i \ \delta Z_i]^T \quad (38)$$

A.3 Functional models

The functional models are for the accelerometer readings given by (see [8]):

$$E(g_x) = -G \sin I \sin \tau \quad (39)$$

$$E(g_y) = -G \sin I \cos \tau \quad (40)$$

$$E(g_z) = G \cos I \quad (41)$$

and for the magnetometer readings:

$$E(b_x) = B(\cos \Theta \cos I \cos A_m \sin \tau + \cos \Theta \sin A_m \cos \tau - \sin \Theta \sin I \sin \tau) \quad (42)$$

$$E(b_y) = B(\cos \Theta \cos I \cos A_m \cos \tau - \cos \Theta \sin A_m \sin \tau - \sin \Theta \sin I \cos \tau) \quad (43)$$

$$E(b_z) = B(\cos \Theta \sin I \cos A_m + \sin \Theta \cos I) \quad (44)$$

where G is the local gravity, B is the strength of the local Earth's magnetic field, A_m the magnetic azimuth, I the inclination and τ the high side toolface. Additional model param-

Detection of Gross Errors in Wellbore Directional Surveying

ters are not taken into consideration here. Note that I and τ are common parameters in all equations.

References

[1] Torgeir Torkildsen, Oddvar Lotsberg “Acceptance values for MWD Magnetic Wellbore Surveying.”, ISCWSA, 2001.
 [2] Karl Rudolf Koch “Parameter Estimation and Hypothesis Testing in Linear Models.” ISBN 3-540-65257-4, Springer-Verlag 1999.
 [3] P.J.G. Teunissen “Testing theory: an introduction.” ISBN 90-407-1975-6, Delft University Press 2000.
 [4] Allen J. Pope “The Statistics of Residuals and the Detection of Outliers.” NOAA Technical Report NOS 65 NGS 1 65, U.S. Department of Commerce, Rockville, USA, Delft University Press 2000.
 [5] Hugh S. Williamson “Accuracy prediction for directional MWD” Paper SPE 67616, SPE Drilling and Completion 15 (4), December 2000.

[6] Weikko A. Heiskanen, Helmut Moritz “Physical Geodesy” San Francisco, W. H. Freeman, c1967.
 [7] Andrew G. Brooks, P.A.Gurden, K.A.Noy “Practical Application of a Multiple-Survey Magnetic Correction Algorithm.” Paper SPE 49060, 1998 SPE Annual Technical Conference and Exhibition, New Orleans, 27 September–30 October 1998.
 [8] Roger Ekseth “Uncertainties in connection with the determination of wellbore positions.” ISBN 82-471-0218-8, Doctoral thesis 1998, Norwegian University of Science and Technology, 1998:24 IPT-rapport.

Footnotes:

- 1 A type I error is the probability of rejecting H_0 when it is true.
- 2 $1-\beta$ is the probability of rejecting H_A when it is true and is often referred to as a type II error.

File translated from T_EX by T_TH, version 3.64. On 22 Dec 2004, 14:49.